

Design of Photo Voltaic System an Application of Phase Shifted Cascaded Multilevel Inverter

Mr. G. Venkateswarlu¹, Dr.P Sangameswar Raju², K.Rakesh³

¹Prof in dept of EEE, Narayana Engg College, Nellore

²Professor, S.V.Univesity, Tirupati.

³Mtech Student Scholar Narayana and Engg. , Nellore A.P, India.

Abstract—A hybrid cascaded multilevel inverter application for renewable energy resources including a reconfiguration technique is developed. Renewable energy resources (RES) have had increasing penetration levels for grid connected distributed generation (DG) in recent years. Photovoltaic, micro-turbine, wind turbine and fuel cell put forward many promising applications with high efficiency and low emissions. Together with power electronics technologies, these have provided an important improvement for RES and DG applications; especially, a micro-grid concept is introduced in to provide more system capacity and control flexibility when several RESs with different electric behaviors are integrated in the same grid. To obtain improved power quality, lower switching losses, better electromagnetic compatibility, and higher voltage capability. The benefits are especially clear for medium-voltage drives in industrial applications. Several topologies for multilevel inverters have been proposed over the years; the most popular cascaded H-bridge apart from other multilevel. This paper presents a single-phase cascaded H-bridge multilevel inverter for a photovoltaic (PV) system.

Keywords—Amplitude modulation (AM), dc-ac power conversion, insulated-gate bipolar transistor (IGBT), power electronics, pulse-width modulation, voltage-source converter (VSC).

I. INTRODUCTION

The Industrial Revolution of the 19th century ushered in new technologies. Some of these inventions involved use of natural resources like coal and oil. The thought of exhaustible nature of these resources and the environmental damage from the use of these resources never occurred either to the inventors or the subsequent generations. In the quest to sustain galloping economic activity, the dependence on coal and oil has soared at a phenomenal rate over the years. The burnt fuels result in the release of carbon dioxide and other gases into the atmosphere causing environmental damage. It has become imperative to look at energy technology with a new perspective. There are abundant renewable sources of energy such as wind, sun, water, sea, biomass apart from even daily wastes. These sources are pollution free and hence clean energy apart from being unlimited/ inexhaustible. Among them solar is more advantageous because the Solar Photo Voltaic (SPV) technology which enables the direct conversion of sun light into electricity can be used to run pumps, lights, refrigerators, TV sets, etc., and it has several distinct advantages, since it does not have moving parts, produces no noise or pollution, requires very little maintenance and can be installed anywhere. A single-phase structure of an m-level cascaded inverter is illustrated in Figure .1. Each separate dc source (SDCS) is connected to a single-phase full-bridge, or H-bridge, inverter. Each inverter level can generate three different voltage outputs, $+V_{dc}$, 0, and $-V_{dc}$ by connecting the dc source to the ac output by different combinations of the four switches, S_1 , S_2 , S_3 , and S_4 . To obtain $+V_{dc}$, switches S_1 and S_4 are turned on, whereas $-V_{dc}$ can be obtained by turning on switches S_2 and S_3 . By turning on S_1 and S_2 or S_3 and S_4 , the output voltage is 0. The ac outputs of each of the different full-bridge inverter levels are connected in series such that the synthesized voltage waveform is the sum of the inverter outputs. The number of output phase voltage levels m in a cascade inverter is defined by $m = 2s+1$, where s is the number of separate dc sources.

II. MODEL FOR PV CELL

The building block of the PV array is the solar cell, which is basically a p-n semiconductor junction that directly converts light energy into electricity. The equivalent circuit is shown in Fig. 4

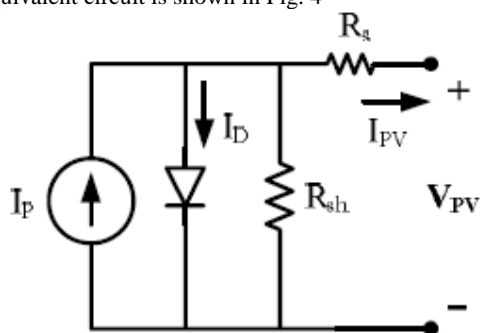


Fig. 1 Equivalent circuit for a PV cell.

To simulate a PV array, a PV simulation model which was used based on the following equation:

$$I_{PV} = n_p I_{ph} - n_p I_{rs} \left[\exp \left(\frac{q}{kTA} \frac{V_{PV}}{n_s} \right) - 1 \right] \quad (1)$$

Where I_{PV} is the PV array output current (A); V_{PV} is the PV array output voltage (V); n_s is the number of cells connected in series; n_p is the number of strings connected in parallel; q is the charge of an electron; k is Boltzmann's constant; A is the p-n junction ideality factor; T is the cell temperature (K); and I_{rs} is the cell reverse saturation current. The factor A in Eq. (1) determines the cell deviation from the ideal p-n junction characteristics. The ideal value ranges between 1 and 5 and in our case, A equals 2.15. The cell reverse saturation current I_{rs} varies with temperature and the photocurrent I_{ph} depends on the solar radiation and the cell temperature as shown in the following equation:

$$I_{ph} = [I_{scr} + k_i(T - T_r)] \frac{s}{100} \quad (2)$$

where I_{scr} is the cell short-circuit current at reference temperature and radiation, k_i is the short-circuit current temperature coefficient, and s is the solar radiation

III. CASCADED H-BRIDGE MULTILEVEL CONVERTER

Full H-Bridge

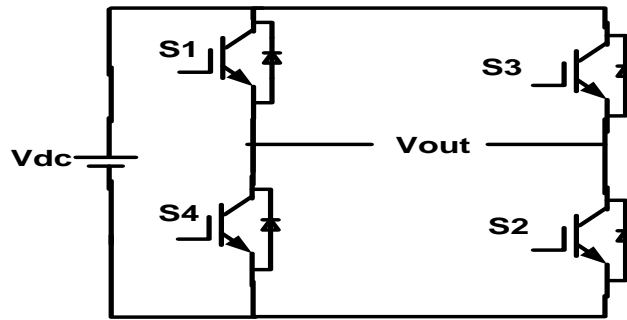


Figure. 2 Full H-Bridge

Switches Turn ON	Voltage Level
S1,S2	Vdc
S3,S4	-Vdc
S4,D2	0

Table 1. Switching table for H-Bridge

Fig.2 shows the Full H-Bridge Configuration. By using single H-Bridge we can get 3 voltage levels. The number output voltage levels of cascaded Full H-Bridge are given by $2n+1$ and voltage step of each level is given by Vdc/n . Where n is number of H-bridges connected in cascaded. The switching table is given in Table 1 and 2.

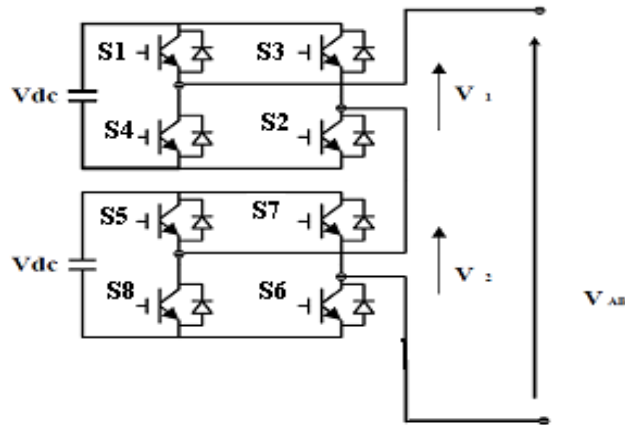


Fig. 3 Cascaded H-Bridge

Table 2. Switching table for Cascaded H-Bridge

Switches Turn On	Voltage Level
S1, S2	Vdc
S1,S2,S5,S6	2Vdc
S4,S6,S8,S6	0
S3,S4	-Vdc
S3,S4,S7,S8	-2Vdc

IV. PHASE SHIFTED PWM METHOD

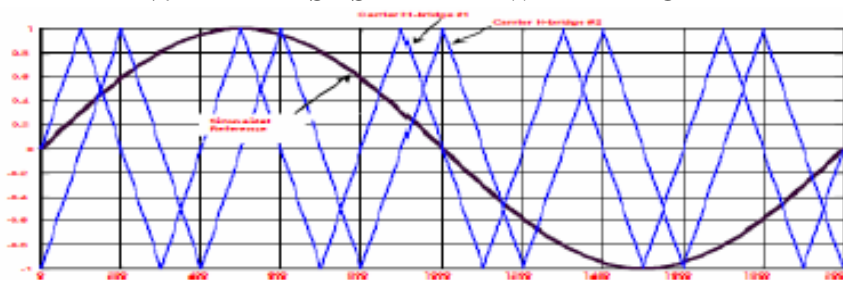


Fig. 3 Phase shifted carrier and reference waves

The Phase shifted carrier pulse width modulation, in general, a multilevel inverter with m voltage levels requires $(m - 1)$ triangular carriers. In the phase shifted multicarrier modulation, all the triangular carriers have the same frequency and the same peak-to-peak amplitude, but there is a phase shift between any two adjacent carrier waves, given by $(360^\circ/(m-1))$. The modulating signal is usually a three-phase sinusoidal wave with adjustable amplitude and frequency. The gate signals are generated by comparing the modulating wave with the carrier waves. It means for the five level inverter, four are triangular carriers are needed with a 90° phase displacement between any two adjacent carriers. In this case the phase displacement of $V_{cr1} = 0^\circ$, $V_{cr2} = 90^\circ$, $V_{cr1-} = 180^\circ$ and $V_{cr2-} = 270^\circ$. B. Incremental Conductance Method

V. SIMULATION RESULTS

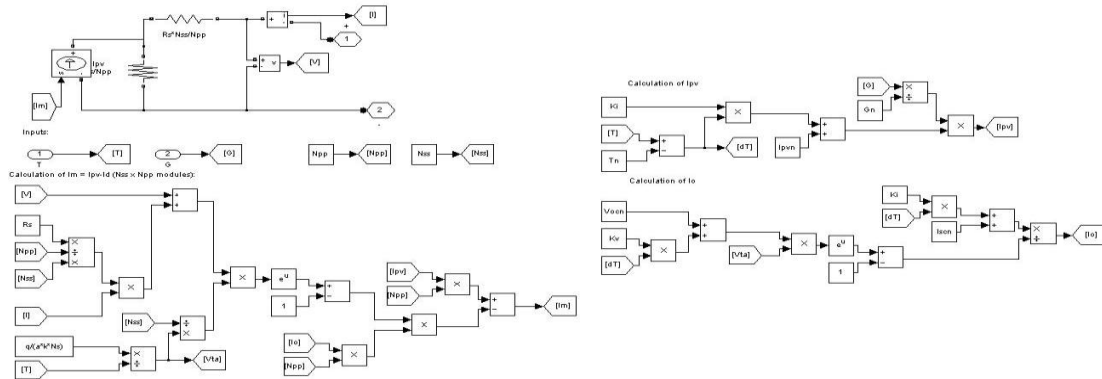


Fig. 4 Simulink model of PV Module

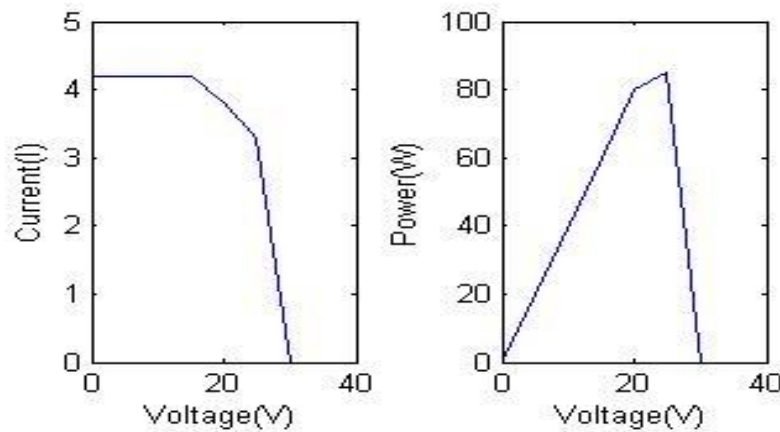


Fig. 5 Characteristics of PV model

Fig.5 shows the SIMULINK model of the PV system and its characteristics are shown in Fig. 5 in which V-I and V-P curves were plotted.

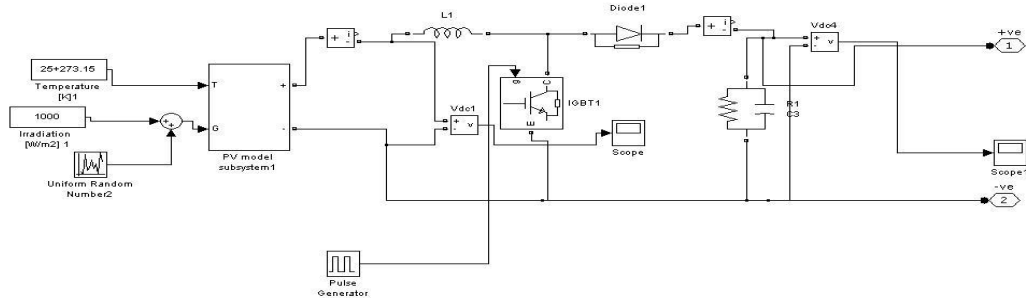


Fig. 6 Matlab simulink model of DC circuit

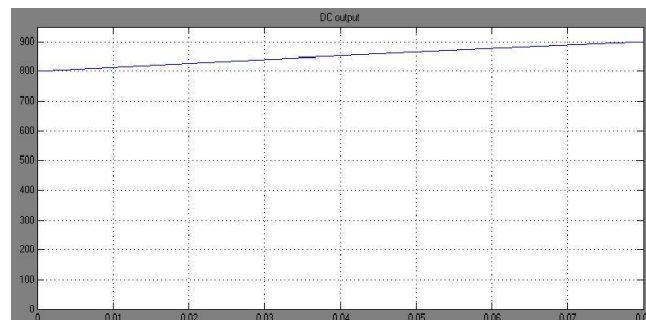


Fig. 7 DC output voltage waveform of DC circuit

Fig.7 is the DC-DC converter simlink model in which the output of the PV system may not provide the constant voltage. The input to the CMI is a constant voltage, in-order to obtain the constant voltage the DC-DC is utilized and the voltage waveform is seen in the Fig. 8.

5.1 Modeling of Cascaded H-Bridge Multilevel Converter

Fig.8 shows the Matlab/Simulink Model of five level Cascaded H-Bridge multilevel converter. Each H-bridge DC voltage is 50 V. In order to generate three phase output such legs are connected in star/delta. Each llege gating pulses are displaced by 120 degrees.

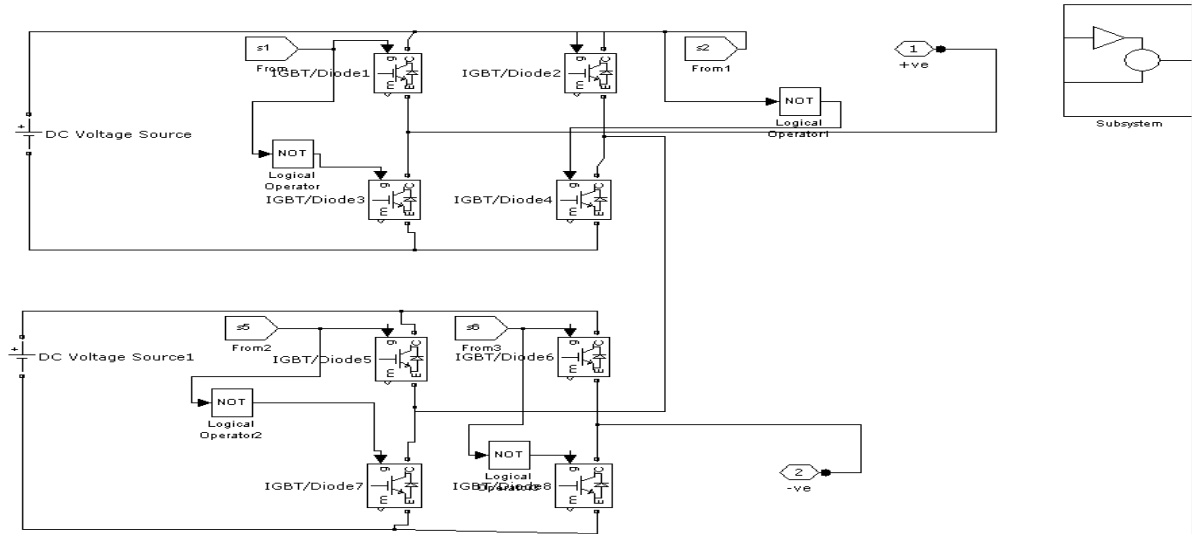


Figure. 8 Matlab/Simulink Model of CHB

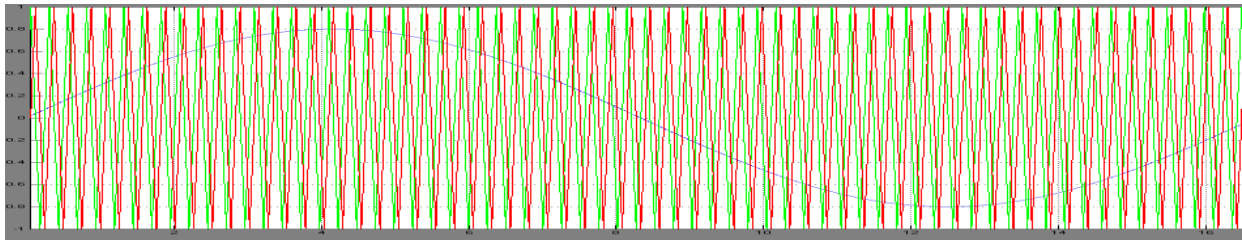


Figure. 9 Carrier Signals of Phase Shifted Carrier PWM

Fig.9 shows the Phase shifted Carrier PWM wave form. Here four carriers each are phase shifted by 90 degrees are compared with sine wave.

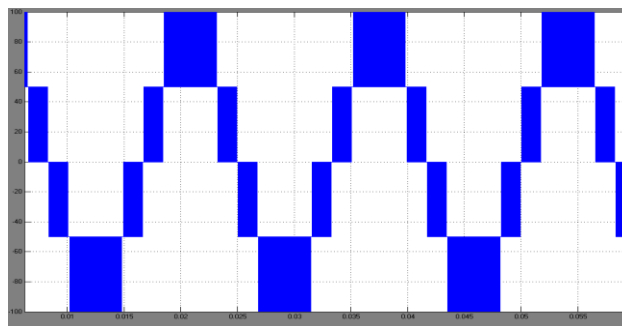


Figure. 10 Five Level output

Fig.10 shows the phase voltage of phase shifted carrier PWM CHB inverter. Fig.11 shows the line voltage of phase shifted carrier PWM CHB inverter. Here phase voltage has five voltage levels where as line voltage has nine voltage levels.

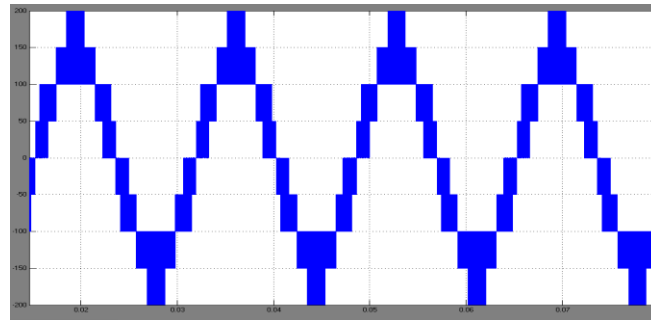


Figure. 11 Nine Level Line Voltage

VI. CONCLUSION

This paper presents a cascaded H-Bridge multilevel inverter connected to the individual photovoltaic sources as a single DC source. The PV system is modeled and its characteristics were plotted. The CMI are controlled with the help of phase shifted PWM method, which is more advantageous method when compared to techniques. A SIMULINK based model is developed and Simulation results are presented.

REFERENCES

- [1]. J. McDonald, "Leader or follower [The business scene]," *IEEE Power Energy Mag.*, vol. 6, no. 6, pp. 18–90, Nov. 2008.
- [2]. N. Flourentzou, V. G. Agelidis, and G. D. Demetriades, "VSC-based HVDC power transmission systems: An overview," *IEEE Trans. Power Electron.*, vol. 24, no. 3, pp. 592–602, Mar. 2009.
- [3]. A. A. Edris, S. Zelingher, L. Gyugyi, and L. J. Kovalsky, "Squeezing more power from the grid," *IEEE Power Eng. Rev.*, vol. 22, no. 6, pp. 4–6, Jun. 2002.
- [4]. B. K. Perkins and M. R. Irvani, "Dynamic modeling of high power static switching circuits in the dq-frame," *IEEE Trans. Power Syst.*, vol. 14, no. 2, pp. 678–684, May 1999.
- [5]. P. Steimer, O. Apeldoorn, E. Carroll, and A. Nagel, "IGCT technology baseline and future opportunities," in *Proc. IEEE Transm. Distrib. Conf. Expo.*, Oct. 2001, vol. 2, pp. 1182–1187.
- [6]. V. G. Agelidis and G. Joos, "On applying graph theory toward a unified analysis of three-phase PWM inverter topologies," in *Proc. IEEE Power Electronics Specialists Conf.*, Seattle, WA, Jun. 1993, pp. 408–415.
- [7]. J. Arrillaga, Y. H. Liu, and N. R. Watson, *Flexible Power Transmission: The HVDC options*. Hoboken, NJ: Wiley, 2007.
- [8]. G. Asplund, "Application of HVDC light to power system enhancement," in *Proc. IEEE Power Eng. Soc. Winter Meeting*, Singapore, Jan. 2000, vol. 4, pp. 2498–2503.
- [9]. P. N. Enjeti, P. D. Ziogas, and M. Ehsani, "Unbalanced PWM converter analysis and corrective measures," in *Proc. IEEE Industry Applications Soc. Annu. Meet.*, San Diego, CA, Oct. 1989, pp. 861–870.
- [10]. P. N. Enjeti and W. Shireen, "A new technique to reject dc-link voltage ripple for inverters operating on programmed PWM waveforms," *IEEE Trans. Power Electron.*, vol. 7, no. 1, pp. 171–180, Jan. 1992.
- [11]. J. Y. Lee and Y. Y. Sun, "Adaptive harmonic control in PWM inverters with fluctuating input voltage," *IEEE Trans. Ind. Electron.*, vol. IE-33, no. 1, pp. 92–98, Feb. 1986.
- [12]. S. Funabiki and Y. Sawada, "Computative decision of pulse width in three-phase PWM inverter," in *Proc. IEEE Industry Applications Soc. Annu. Meet.*, Pittsburgh, PA, Oct. 1988, pp. 694–699.
- [13]. T. Kato, "Precise PWM waveform analysis of inverter for selected harmonic elimination," in *Proc. IEEE Industry Appl. Soc. Annu. Meeting*, Piscataway, NJ, Sep. 1986, vol. 1, pp. 611–616.
- [14]. B. P. McGrath and D. G. Holmes, "A general analytical method for calculating inverter dc-link current harmonics," in *Proc. IEEE Ind. Appl. Soc. Annu. Meeting*, Edmonton, AB, Canada, Oct. 2008, pp. 1–8.
- [15]. A. M. Cross, P. D. Evans, and A. J. Forsyth, "DC link current in PWM inverters with unbalanced and nonlinear loads," *Proc. Inst. Elect. Eng., Elect. Power Appl.*, vol. 146, no. 6, pp. 620–626, Nov. 1999.
- [16]. M. H. Bierhoff and F. W. Fuchs, "DC-link harmonics of three-phase voltage-source converters influenced by the pulsewidth-modulation strategy—An analysis," *IEEE Trans. Ind. Electron.*, vol. 55, no. 5, pp. 2085–2092, May 2008.
- [17]. M. N. Anwar and M. Teimor, "An analytical method for selecting dc-link-capacitor of a voltage stiff inverter," in *Proc. 37th IAS Annu. Meeting IEEE Industry Applications Conf.*, Dearborn, MI, Oct. 2002, vol. 2, pp. 803–810.
- [18]. F. D. Kieferndorf, M. Forster, and T. A. Lipo, "Reduction of dc-bus capacitor ripple current with PAM/PWM converter," *IEEE Trans. Ind. Appl.*, vol. 40, no. 2, pp. 607–614, Mar. 2004.
- [19]. P. N. Enjeti, P. D. Ziogas, and J. F. Lindsay, "Programmed PWM techniques to eliminate harmonics: A critical evaluation," *IEEE Trans. Ind. Appl.*, vol. 26, no. 2, pp. 302–316, Mar. 1990.
- [20]. V. G. Agelidis, A. Balouktsis, I. Balouktsis, and C. Cossar, "Multiple sets of solutions for harmonic elimination PWM bipolar waveforms: Analysis and experimental verification," *IEEE Trans. Power Electron.*, vol. 21, no. 2, pp. 415–421, Mar. 2006.
- [21]. L. Ran, L. Holdsworth, and G. A. Putrus, "Dynamic selective harmonic elimination of a three-level inverter used for static VAR compensation," *Proc. Inst. Elect. Eng., Gen., Transm. Distrib.*, vol. 149, no. 1, pp. 83–89, Jan. 2002.

- [22]. S. Filizadeh and A. M. Gole, "Harmonic performance analysis of an OPWM-controlled STATCOM in network applications," *IEEE Trans. Power Del.*, vol. 20, no. 2, pt. 1, pp. 1001–1008, Apr. 2005.
- [23]. C. Hochgraf and R. H. Lasseter, "Statcom controls for operation with unbalanced voltages," *IEEE Trans. Power Del.*, vol. 13, no. 2, pp. 538–544, Apr. 1998.
- [24]. B. Blazic and I. Papic, "Improved D-STATCOM control for operation with unbalanced currents and voltages," *IEEE Trans. Power Del.*, vol. 21, no. 1, pp. 225–233, Jan. 2006.